ISSN: 2447-3359

REVISTA DE GEOCIÊNCIAS DO NORDESTE

Northeast Geosciences Journal

v. 12, nº 1 (2026)

https://doi.org/10.21680/2447-3359.2026v12n1ID40279

Evaluation of the geometric quality of point clouds generated by smartphone

Avaliação da qualidade geométrica de nuvens de pontos geradas por smartphone

Victor Lachini Cola[1] ; Laura Coelho de Andrade[2] ; Nilcilene das Graças Medeiro [3]; Afonso de Paula dos Santos[4]; Wiliam Rodrigo Dal Poz[5]; Italo Oliveira Ferreira[6]

[1] Federal University of Viçosa, Department of Civil Engineering, Viçosa, MG, Brazil. Email: victor.lachini@hotmail.com
ORCID: https://orcid.org/0009-0001-7761-3193
[2] Federal University of Viçosa, Department of Civil Engineering, Viçosa, MG, Brazil. Email: laura.andrade@ufv.br
ORCID: https://orcid.org/0000-0003-3693-2208
[3] Federal University of Viçosa, Department of Civil Engineering, Viçosa, MG, Brazil. Email: nilcilene.medeiros@ufv.br
ORCID: https://orcid.org/0000-0003-0839-3729
[4] Federal University of Viçosa, Department of Civil Engineering, Viçosa, MG, Brazil. Email: afonso.santos@ufv.br
ORCID: https://orcid.org/0000-0001-7248-4524
[5] Federal University of Viçosa, Department of Civil Engineering, Viçosa, MG, Brazil. Email: william.dalpoz@ufv.br
ORCID: https://orcid.org/0000-0001-9532-3643
[6] Federal University of Viçosa, Department of Civil Engineering, Viçosa, MG, Brazil. Email: italo.ferreira@ufv.br
ORCID: https://orcid.org/0000-0002-4243-8225

Abstract: 3D modeling is a widely used tool for the analysis of three-dimensional data, offering greater accuracy and detail of the objects studied. Among the technologies employed, LiDAR (Light Detection and Ranging) stands out for its ability to generate higher-quality point clouds through laser scanning. With technological advances, smartphones equipped with LiDAR sensors, such as the Apple iPhone 14 Pro, provide greater flexibility and productivity compared to traditional equipment. Thus, this study evaluated the geometric quality of 3D point clouds generated by the smartphone's LiDAR sensor and by close-range photogrammetry. The case study focused on the façade of the Surveying and Cartographic Engineering Laboratory, located on the campus of the Federal University of Viçosa, in Viçosa – MG, Brazil. Measurements obtained with a Total Station were used as reference for the geometric quality analysis. The results indicated that, for small objects, close-range photogrammetry showed better performance in terms of geometric definition. On the other hand, for larger areas, such as a building façade, the LiDAR system demonstrated superiority in the geometric quality of the generated point clouds. This study shows that the choice of the most suitable technology depends on the size and characteristics of the analyzed object, highlighting the potential of smartphones equipped with LiDAR sensors for specific applications in three-dimensional data acquisition.

Keywords: 3D Modeling; LiDAR; Photogrammetry; Geometric Quality.

Resumo: A modelagem 3D é uma ferramenta amplamente utilizada para análise de dados tridimensionais, oferecendo melhor precisão e detalhamento dos objetos estudados. Entre as tecnologias empregadas, o LiDAR (Light Detection and Ranging) destaca-se por sua capacidade de gerar nuvens de pontos de melhor qualidade por meio de varredura a laser. Com o avanço tecnológico, smartphones equipados com sensores LiDAR, como o Apple iPhone 14 Pro, oferecem maior flexibilidade e produtividade em comparação aos equipamentos tradicionais. Assim, a presente pesquisa avaliou a qualidade geométrica das nuvens de pontos 3D geradas pelo sensor LiDAR do smartphone e por fotogrametria de curta distância. O estudo de caso foi a fachada do Laboratório de Engenharia de Agrimensura e Cartográfica, no campus da Universidade Federal de Viçosa, em Viçosa – MG. As medições obtidas com uma Estação Total foram usadas como referência para a análise da qualidade geométrica.Os resultados indicaram que, para objetos de pequenas dimensões, a fotogrametria de curta distância apresentou melhor desempenho em termos de definição geométrica. Por outro lado, para áreas maiores, como a fachada de um prédio, o sistema LiDAR mostrou superioridade na qualidade geométrica das nuvens de pontos geradas. Este trabalho demonstra que a escolha da tecnologia mais adequada depende do tamanho e das características do objeto analisado, ressaltando o potencial de smartphones equipados com sensores LiDAR para aplicações específicas na obtenção de dados tridimensionais.

Palavras-chave: Modelagem 3D; LiDAR; Fotogrametria; Qualidade Geométrica.

Received: 22/05/2025; Accepted: 10/04/2026; Published: 24/04/2026.

1. Introduction

In recent years, the use of mobile devices such as smartphones and tablets has become increasingly common and accessible. Some of these devices are equipped with sensors capable of capturing three-dimensional information from the environment, using a Laser source (Light Amplification by Stimulated Emission of Radiation), resulting in the generation of 3D point clouds.

Three-dimensional information can be obtained in various ways, through topographic surveys or using other indirect data collection techniques, such as photogrammetry and LiDAR (Light Detection and Ranging – airborne laser scanning). Such information constitutes three-dimensional point clouds that serve as the basis for generating three-dimensional modeling (BECKER; CENTENO, 2013, p. 652). It is also worth highlighting the work developed by Silva et al. (2024, p. 285), in which the authors evaluated the quality and accuracy of terrestrial laser scanner (TLS) data in a flat area of the Federal University of Viçosa, in Viçosa-MG. More recent research by Sawandi et al. (2026) considered the potential of smartphones as 3D mapping devices, applied to participatory planning and the production of localized spatial data, focusing on two main types of sensors, namely LiDAR and standard RGB cameras, where the authors evaluated performance in generating 3D models. Considering the current state of the art, it is also important to highlight the research by Tomczak et al. (2026), in which the authors estimated the volume of stacked wood using a dynamic conversion factor calculated by a smartphone application based on LiDAR.

Three-dimensional models provide spatial information of great importance for the modeling and analysis of the Earth's surface. These are considered essential inputs for obtaining information on distances, areas, and volumes, among other applications (MICELI, 2011, p. 192).

Studies involving iPhones equipped with LiDAR sensors, such as that developed by Luetzenburg et al. (2021, p. 2), considered a series of experiments to evaluate the performance of the iPhone 12 Pro for engineering applications. The authors used the iPhone to measure various objects, including trees, buildings, and terrain, comparing the results with those obtained from other LiDAR systems. They found that the iPhone was capable of providing accurate measurements for these objects, with an accuracy between 0.5–1.5 cm. The iPhone performed particularly well when measuring flat surfaces and objects with clear features, such as buildings. However, it showed lower performance when measuring objects with complex shapes or rough surfaces, such as rocks and terrain (SULEYMANOGLU, 2023, p. 351). In addition, Gonçalves and Albarici (2025, p. 1261) evaluated the accuracy of point clouds generated by smartphones equipped with LiDAR technology and concluded that these devices are capable of producing digital terrain models with sufficient accuracy for applications in most engineering and geoscience works, providing an accessible and convenient alternative compared to topographic laser scanning surveys. In terms of the state of the art and international research, it is also worth highlighting the publication by Janicka and Błaszczak-Bąk (2025, p. 18), in which the authors conducted comparative tests between LiDAR embedded in smartphones and TLS data, obtaining differences on the order of centimeters.

Unlike the well-established LiDAR technology, which uses high-quality inertial sensors mounted on airborne platforms, the influence on the geometric quality of point clouds generated by inertial sensors embedded in smartphones remains a relatively underexplored aspect to date. Data acquisition using these devices presents limitations, highlighting the importance of evaluating not only the inertial sensor but also other factors that may influence the geometric quality of the generated point clouds and their respective products.

Smartphones also provide the opportunity to capture photographs of any object, at any time and instantly, enabling their use in the domain of digital photogrammetry (FAWZY, 2015, p. 77). Three-dimensional modeling from multiple photographs taken from different viewing angles of objects close to the sensor is a branch of close-range photogrammetry that plays a fundamental role in data collection and storage, as well as in the generation of products such as 3D models.

With the continuous improvement of physical components (hardware) and the ongoing development of robust camera systems that integrate them (GOMES, 2021, p. 3), a new way of acquiring data has emerged. These devices are becoming increasingly advanced, enabling more efficient and accurate collection of 3D information.

Through Cartographic Quality Control, aspects such as geometric accuracy, topological integrity, and consistency of the 3D models obtained from smartphones are analyzed. In summary, Cartographic Quality Control plays a role in evaluating and improving the quality of products generated by 3D modeling techniques available through the use of smartphones.

In this context, the objective of this study is to assess the geometric quality of 3D point clouds generated using the Apple iPhone 14 Pro device (APPLE, 2023) for performing 3D modeling tasks. Furthermore, the research also identifies possible limitations of the iPhone 14 Pro LiDAR sensor by evaluating the geometric quality of point clouds and surfaces.

2. Methodology

2.1 Study Area and Materials

Initial experiments were conducted using small-scale geometric objects in a more controlled context, in order to evaluate the performance of the inertial sensor in generating the 3D point cloud, in comparison with the 3D point cloud generated based on the principle of stereoscopy, through close-range photogrammetry.

After the initial experiments, a study area was selected in an environment with larger geometric proportions, aiming to analyze the potential of two approaches: 3D point cloud generation using an inertial sensor and 3D point cloud generation using stereoscopy. The experiment was carried out on the campus of the Federal University of Viçosa, in Viçosa – MG. The study area corresponded to the façade of the Laboratory of Surveying and Cartographic Engineering (LEA), as shown in Figure 1.

Figure 1 – LEA building facade.
Source: Authors (2026).

The facade was selected as the study area due to its ease of access and its suitability for simulating common cartographic applications, such as urban cadastral surveys of residential buildings. Strategic points were defined across the facade to enable measurements using a total station. In addition, elements present on the facade, such as windows and doors, were adopted as reference features and were also measured with the total station due to their clear visibility and regular geometry. This approach enabled the acquisition of well-defined and representative data for subsequent analysis and evaluation.

An iPhone 14 Pro was employed, equipped with a high-resolution camera system (2× 12 MP and 48 MP sensors, 48 mm and 24 mm focal lengths, f/1.78 aperture, sensor-shift optical image stabilization, and a seven-element lens) and an integrated LiDAR sensor (APPLE, 2023). Furthermore, a Geodetic GD2i-8 total station (CPE, 2023) was used to obtain distance and angle measurements between reference points, while a ZAAS digital caliper was used to acquire measurements of smaller objects. These measurements were subsequently compared with those obtained from LiDAR and close-range photogrammetry.

2.2 Methods

In an initial stage, experiments were conducted using small-scale objects with different shapes and colors (Figure 2). These elements were scanned using the LiDAR sensor, and photographs were acquired from multiple viewing angles of the geometric objects (Figure 3). The objects included a polystyrene sphere of approximately 15 cm in diameter in different

colors (blue, red, and green), as well as a cube with faces painted in distinct colors. The adjustable parameters include confidence, which represents the amount of data received by the sensor; depth, which indicates the limited scanning range; masking, which isolates the predominant object; and point cloud resolution.

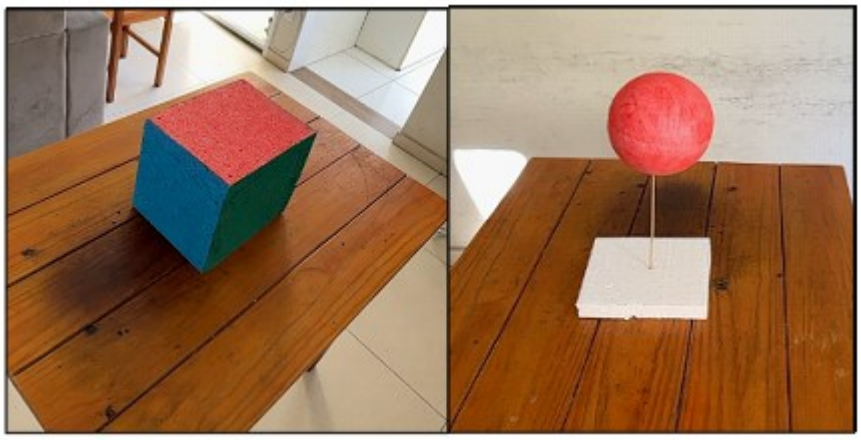

Figure 2 – Scanned polystyrene spheres and cube.
Source: Authors (2026).

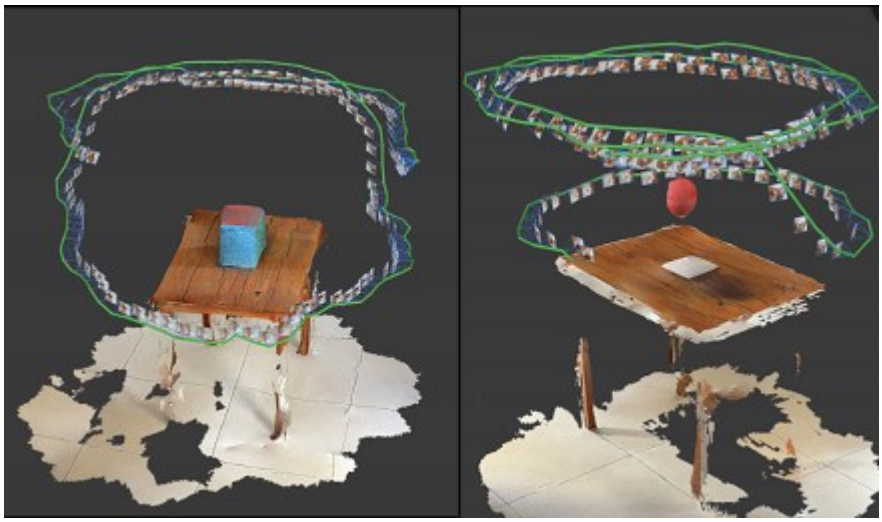

Figure 3 – iPhone 14 Pro trajectory.
Source: Authors (2026).

Following the initial experiments with circular and quadrangular objects, experiments were conducted in the study area, involving surveys of the LEA building facade using both the iPhone and a total station. A Geodetic GD2i-8 total station was used, applying conventional topographic surveying techniques to obtain measurements from points of interest. Subsequently, the facade was surveyed using the iPhone 14 Pro and the "3D Scanner App" (AI PHOTO Editor Lab, 2024, Figure 4) in LiDAR mode, with the parameters set to "High confidence," "5.0 m range," "masking disabled," and "50 mm high resolution."

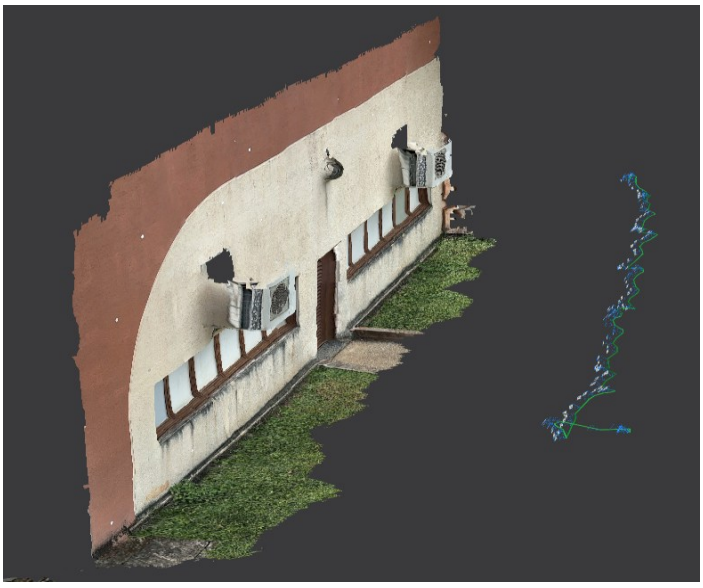

Figure 4 – Illustration of the study area survey using the iPhone.
Source: Authors (2026).

Finally, the facade survey was performed using the close-range photogrammetric technique, which does not require parameter adjustments by the user, as all processing is carried out within the application using the Scan Mode function, in Photos mode. The workflow presented in Figure 5 illustrates the methodology adopted.

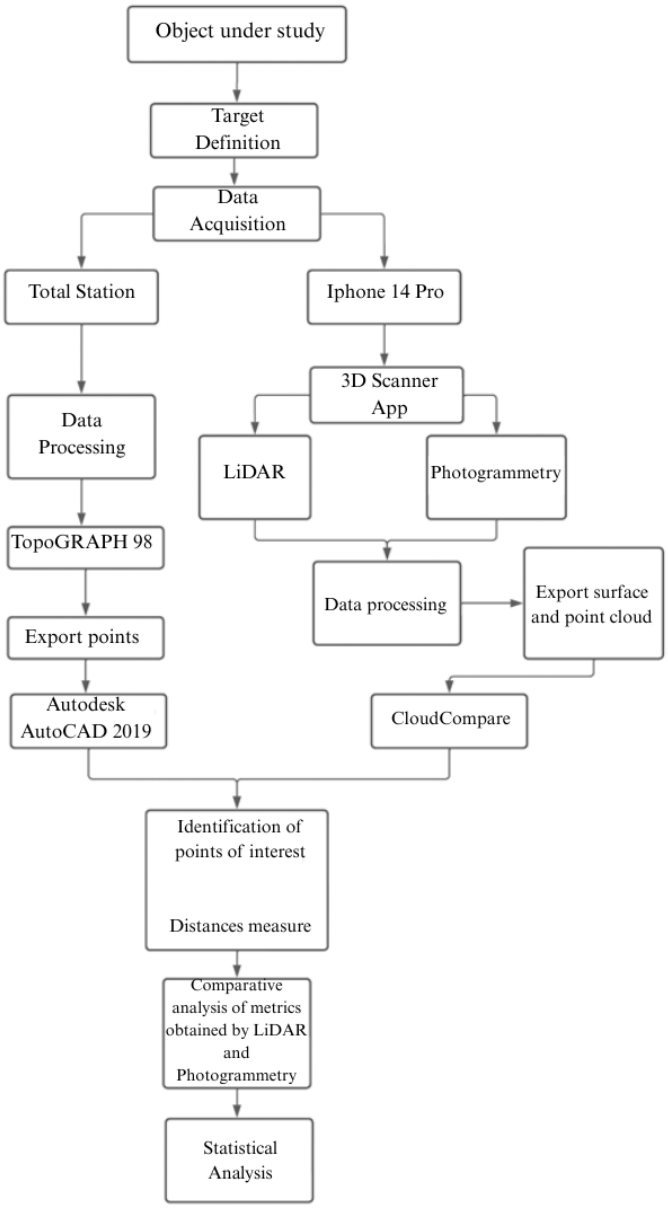

Figure 5 – Workflow for the study area.
Source: Authors (2026).

With the collected data, the processing procedures were carried out. In the case of the reference data obtained using the total station, the Topograph 98 software was used to download the data from the instrument. Subsequently, the data were converted for use in Autodesk AutoCAD 2019, allowing the extraction of the distances of interest. For the first experiment, reference data were obtained using a caliper for the sphere and a scale ruler for the cube.

After data acquisition with the iPhone 14 Pro, both the point cloud file and the surface generated by the application were exported. Subsequently, using CloudCompare (CLOUDCOMPARE, 2023), the files were opened, enabling measurements to be performed on both the point cloud and the generated surface. These procedures provided the results of this study. It is noteworthy that the photogrammetric processing for absolute orientation was performed using navigation data from the IMU (Inertial Measurement Unit). Therefore, the data collected with the total station were used solely as reference for comparison between the two methods (LiDAR and photogrammetry).

Subsequently, planimetric discrepancies were computed. For this purpose, the difference between the reference measurement obtained with the total station and the measurements obtained from the LiDAR and photogrammetric methods was calculated (Equation 1).

$$d = l_o - l_e \tag{1}$$

Where $l_o$is the measurement obtained through the selected method and $l_e$is the measurement obtained from the total station, caliper, or scale ruler.

Statistical procedures were then applied to analyze the data derived from the study area. In this context, descriptive statistics were used, including mean, standard deviation, RMS (Root Mean Square), maximum value, and minimum value. In contrast, for the data derived from the scanned objects, the analysis focused on the evaluation of absolute error.

The arithmetic mean (Equation 2) consists of summing all values of the variable and dividing by the number of observations involved in the sum (CAZORLA, 2003, p. 2).

$$\bar{x} = \frac{\sum x}{n} \tag{2}$$

Where x represents the variable values and $n$is the number of observations.

The standard deviation (Equation 3) is a measure that allows the evaluation of the degree of dispersion of the variable values in relation to the mean. The standard deviation $s$corresponds to the square root of the variance, where the variance is the mean of the squared deviations (OLIVEIRA, 2011).

$$s = \sqrt{\frac{\sum_{i=1}^{n}(x_i - \bar{x})^2}{n}} \tag{3}$$

Where $\bar{x}$is the sample mean and $n$is the number of sample elements.

In data analysis, standard deviation is the most commonly used measure of dispersion, especially in descriptive analyses. This is because it considers all values of the variable while being expressed in the same measurement units (OLIVEIRA, 2011, p. 23).

The RMS (Root Mean Square) is a measure of precision proposed by Gauss. In practical terms, it evaluates the external precision of the data, representing both the tendency and dispersion of the sample in relation to more accurate reference data (SANTOS, 2010, p. 42). It can be calculated according to Equation (4):

$$RMS = \sqrt{\frac{\sum_{i=1}^{n}(x_i)^2}{n}} \tag{4}$$

Where RMS represents the square root of the mean of the squared values. It is used to quantify the precision of a dataset relative to a reference value or estimate. The higher the RMS value, the lower the accuracy of the data.

The relative error (Equation 5) is expressed as the uncertainty in a measurement and can be used to represent measurement imprecision (HELMENSTINE, 2020). Error is defined as the deviation of a measured result from the true value of a measurable quantity, expressed in absolute or relative terms. If A is the true value and $A'$is the measured value, then the difference between A and A'defines the relative error (RABINOVICH, 2006, p. 13).

$$E(\%) = \left|\frac{A' - A}{A}\right| * 100 \quad (5)$$

The smaller the relative error value, the closer the measurement or estimate is to the true value, indicating better precision or accuracy.

3. Results and Discussion

In order to evaluate and compare the results of the proposed strategies, two sets of measurements were performed. The first set consisted of 10 measurements conducted across the study area using a total station in reflectorless measurement mode. The second set of measurements was carried out on the objects presented (Figure 2), using a caliper and a scale ruler. The values obtained from both methods, along with the corresponding study objects, were recorded and are presented in Tables 1 to 6, together with their respective discrepancies.

Table 1 – Distances and discrepancies obtained using LiDAR for the study area.

	LiDAR			**DISCREPANCY**	
LINES	**POINT CLOUD (m)**	**GENERATED SURFACE (m)**	**TOTAL STATION (m)**	**S-E (cm)**	**N-E (cm)**
D1	1.982	1.992	1.964	2.8	1.8
D2	1.213	1.201	1.185	1.6	2.8
D3	3.271	3.273	3.237	3.6	3.4
D4	3.208	3.196	3.237	-4.1	-2.9
D5	4.312	4.315	4.293	2.2	1.9
D6	1.007	1.021	1	2.1	0.7
D7	0.978	1.007	0.992	1.5	-1.4
D8	4.597	4.618	4.598	2	-0.1
D9	0.968	0.982	0.992	-1	-2.4
D10	2.093	2.102	2.106	-0.4	-1.3

Source: Authors (2026).

Table 2 – Distances and discrepancies obtained using photogrammetry for the study area.

	PHOTOGRAMMETRY			DISCREPANCY	
LINES	**POINT CLOUD (m)**	**GEN. SURFACE (m)**	**TOTAL STATION (m)**	**S-E (cm)**	**N-E (cm)**
D1	1.821	1.822	1.964	-14.2	-14.3
D2	1.098	1.091	1.185	-9.4	-8.7
D3	2.942	2.964	3.237	-27.3	-29.5
D4	2.982	2.99	3.237	-24.7	-25.5
D5	3.973	3.982	4.293	-31.1	-32
D6	0.944	0.922	1	-7.8	-5.6
D7	0.923	0.92	0.992	-7.2	-6.9
D8	4.231	4.258	4.598	-34	-36.7
D9	0.914	0.914	0.992	-7.8	-7.8

Source: Authors (2026).

Where S, E, and N represent the generated surface, total station, and point cloud, respectively.

Table 3 – Distances and discrepancies derived from LiDAR for the cube.

	LiDAR BLOCK			DISCREPANCY	
	POINT CLOUD (cm)	**GEN. SURFACE (cm)**	**CALIPER (cm)**	**S-ES (cm)**	**N-ES (cm)**
D1	23.021	22.71	25.4	-2.69	-2.379
D2	18.144	18.55	20.5	-1.95	-2.356
D3	21.742	21.97	22.7	-0.73	-0.958

Source: Authors (2026).

Table 4 – Distances and discrepancies derived from photogrammetry for the cube.

	PHOTOGRAMMETRY BLOCK			DISCREPANCY	
	POINT CLOUD (cm)	**GEN. SURFACE (cm)**	**CALIPER (cm)**	**S-ES (cm)**	**N-ES (cm)**
D1	24.903	25.79	25.4	0.39	-0.497
D2	20.724	21.14	20.5	0.64	0.224
D3	23.202	23.18	22.7	0.48	0.502

Source: Authors (2026).

Where D1, D2, and D3 represent the length, width, and height of the cube, respectively, and ES denotes the scale ruler.

Table 5 – Diameter and discrepancies derived from LiDAR for the sphere

	LiDAR SPHERE			DISCREPANCY	
	POINT CLOUD (cm)	**GEN. SURFACE (cm)**	**CALIPER (cm)**	**S-P (cm)**	**N-P (cm)**
DIAMETER	12.775	12.8	14.879	-2.079	-2.104

Source: Authors (2026).

Table 6 – Diameter and discrepancies derived from photogrammetry for the sphere.

	PHOTOGRAMMETRY SPHERE			DISCREPANCY	
	POINT CLOUD (cm)	**GEN. SURFACE (cm)**	**CALIPER (cm)**	**S-P (cm)**	**N-P (cm)**
DIAMETER	15.47	15.418	14.879	0.539	0.591

Source: Authors (2026).

The discrepancies in the measurements are illustrated in the following graphs.

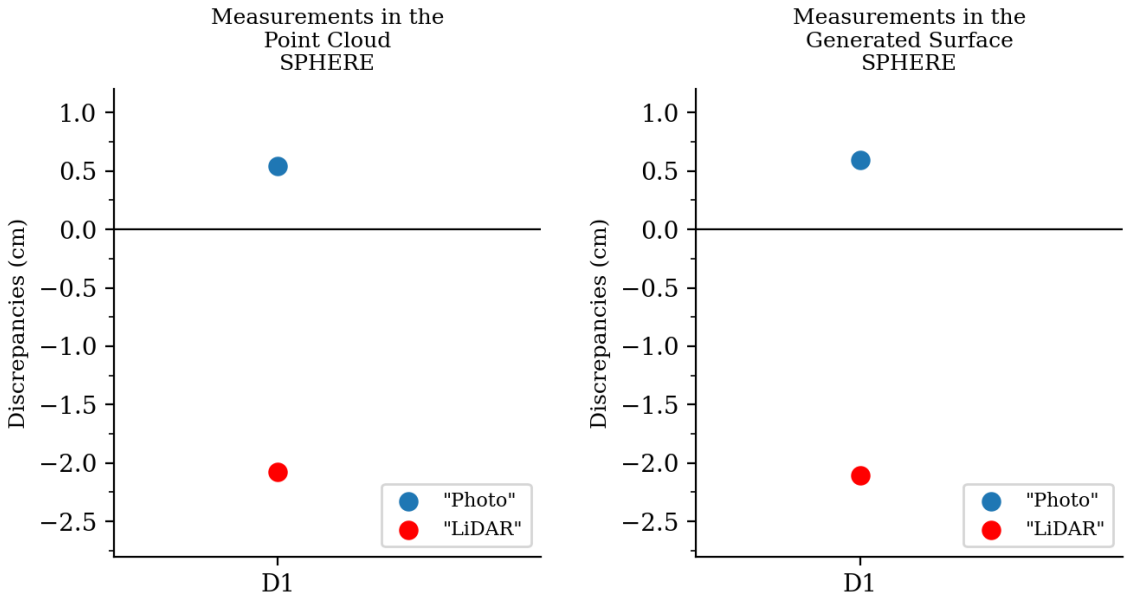

Figure 6 – Discrepancy plot for the sphere.
Source: Authors (2026).

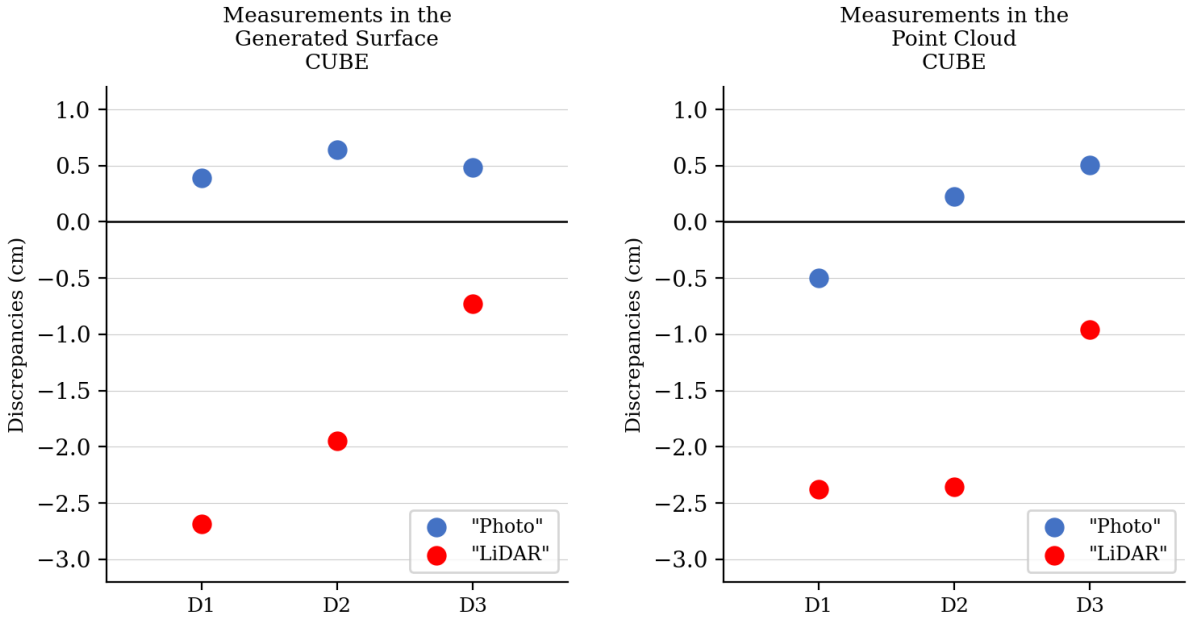

Figure 7 – Discrepancy plot for the cube.
Source: Authors (2026).

Based on Figures 6 and 7, it can be observed that the measurements performed on the surface generated through the photogrammetric method show greater agreement with the reference measurements.

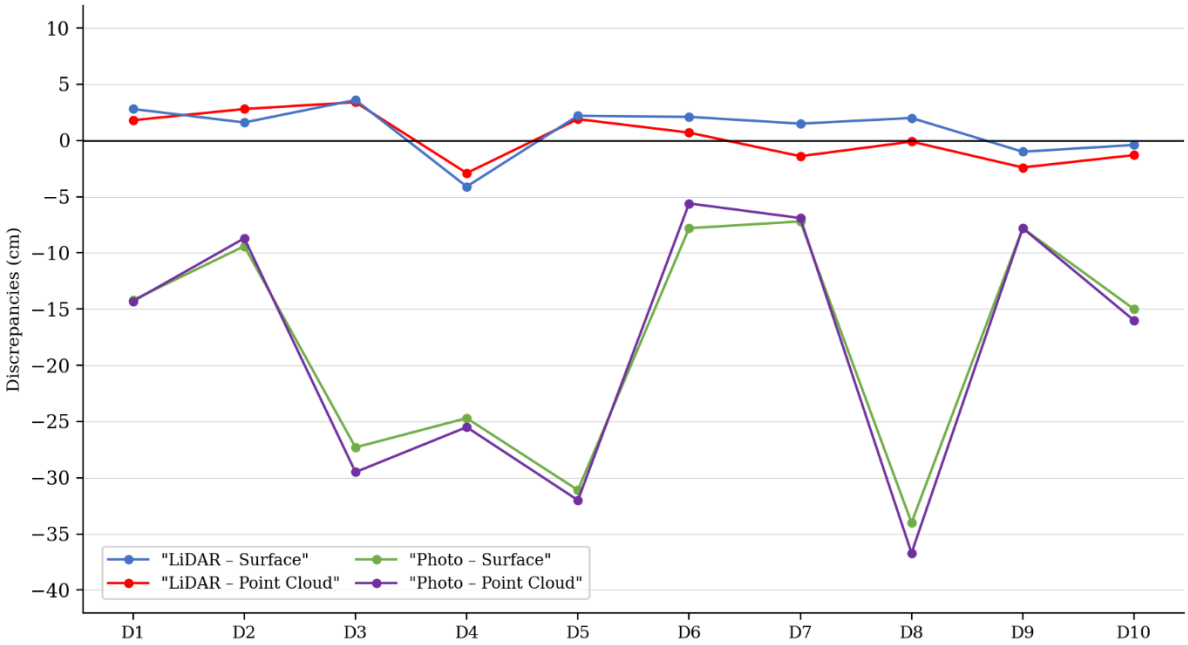

Figure 8 – Discrepancy plot for the study area.
Source: Authors (2026).

As shown in Figure 8, the discrepancies in both the point cloud and the surface generated by the LiDAR method exhibit

smaller differences relative to the reference measurements. It can also be noted that some discrepancies in the point cloud are smaller than those observed in the surface generated by the same method, indicating that measurements performed on the LiDAR point cloud are those that most closely match the reference.

Following the calculation of discrepancies, statistical analyses were performed, and the results are presented in Tables 7 to 11.

Table 7 – Percentage error for the sphere.

	LiDAR		PHOTO	
DIAMETER	**POINT CLOUD**	**GEN. SURFACE**	**POINT CLOUD**	**GEN. SURFACE**
D1	14.14%	13.97%	3.97%	3.62%

Source: Authors (2026).

Table 8 – Percentage error for the cube.

	LiDAR		PHOTO	
DISTANCE	**POINT CLOUD**	**GEN. SURFACE**	**POINT CLOUD**	**GEN. SURFACE**
D1	9.37%	10.59%	1.96%	1.54%
D2	11.49%	9.51%	1.09%	3.12%
D3	4.22%	3.22%	2.21%	2.11%

Source: Authors (2026).

Table 9 – Percentage error for the facade.

	LiDAR		PHOTO	
DISTANCE	**POINT CLOUD**	**GEN. SURFACE**	**POINT CLOUD**	**GEN. SURFACE**
D1	0.92%	1.43%	7.28%	7.23%
D2	2.36%	1.35%	7.34%	7.93%
D3	1.05%	1.11%	9.11%	8.43%
D4	0.90%	1.27%	7.88%	7.63%
D5	0.44%	0.51%	7.45%	7.24%
D6	0.70%	2.10%	5.60%	7.80%
D7	1.41%	1.51%	6.96%	7.26%
D8	0.02%	0.43%	7.98%	7.39%
D9	2.42%	1.01%	7.86%	7.86%
D10	0.62%	0.19%	6.84%	7.17%

Source: Authors (2026).

Table 10 – Statistical metrics for the cube.

	LiDAR		PHOTO	
	POINT CLOUD (cm)	**GEN. SURFACE (cm)**	**POINT CLOUD (cm)**	**GEN. SURFACE (cm)**
Mean	-1.898	-1.79	0.076	0.503
Std. Dev.	0.814	0.99	0.516	0.127
RMS	2.011	1.964	0.428	0.514
Maximum	-0.958	-0.73	0.502	0.64
Minimum	-2.379	-2.69	-0.497	0.39

Source: Authors (2026).

Table 11- Statistical metrics for the facade.

	LiDAR		PHOTO	
	POINT CLOUD (cm)	**GEN. SURFACE (cm)**	**POINT CLOUD (cm)**	**GEN. SURFACE (cm)**
Mean	0.25	1.03	-18.14	-17.86
Std. Dev.	2.21	2.27	11.68	10.44
RMS	2.11	2.38	21.26	20.42
Maximum	3.4	3.6	-5.6	-7.2
Minimum	-2.9	-4.1	-36.7	-34

Source: Authors (2026).

After presenting the obtained results, it can be observed that the photogrammetric method is more suitable when the objects in the scene to be scanned have small dimensions, that is, when the sensor is positioned closer to the objects. Additionally, the higher overlap of the object from multiple viewing angles and perspectives allows for a greater level of detail due to the established geometry. This is evidenced by the standard deviation, RMS, and discrepancy values presented in Tables 10 and 12. Both the point cloud and the generated surface showed satisfactory performance; however, the surface yielded better results compared to the point cloud. Therefore, the use of this method is recommended for applications involving objects with smaller metric proportions located closer to the camera.

On the other hand, when the scene to be scanned is larger, as in the case of the study area considered in this work, the most effective method is the use of the LiDAR sensor. This is supported by the standard deviation, RMS, and discrepancy values presented in Tables 3, 4, and 13. For surveys in this context, the use of the LiDAR sensor with the parameters indicated in Table 2 is recommended, as well as performing the measurements of interest directly on the generated point cloud.

By analyzing the results, particularly the RMS values, it is possible to observe that the measurements obtained using the LiDAR system performed, on average, approximately eight times better than the photogrammetric measurements when evaluated on the generated surface, and approximately ten times better when evaluated on the point cloud.

However, when considering measurements of smaller objects, the close-range photogrammetric method performs better, being, on average, approximately four times more accurate than the LiDAR method.

4. Conclusions

Overall, the data obtained using the iPhone provided interesting results in both experiments conducted. Considering that this sensor is relatively recent, its potential for further improvement is evident.

Based on this study, it can be concluded that the size of the scene to be surveyed is a key factor influencing the choice of the method to be employed, followed by the shape of the object. The methodology adopted proved to be appropriate for evaluating the iPhone 14 Pro and analyzing the acquired data.

When the objects in the scene are smaller and located closer to the acquisition device, the close-range photogrammetry technique proved to be more suitable than laser scanning. Conversely, for larger objects and environments, the LiDAR

approach provided significantly better results, on the order of approximately 8 to 10 times better than the photogrammetric technique.

Based on the obtained results, it is possible to use the selected device for data acquisition, eliminating the need to acquire specific equipment for each application. This clearly demonstrates that technological advances are rendering some traditional practices and instruments used in topographic surveys obsolete for certain applications, particularly those that do not require high precision.

The integration of emerging technologies, such as LiDAR sensors embedded in mobile devices, digital photogrammetry, artificial intelligence, and augmented reality, represents a promising pathway for the advancement of three-dimensional surveying. The combination of these approaches tends to enhance the generation of geospatial products with good spatial, spectral, and temporal resolution, as well as to automate processing and analysis stages, expanding the range of applications—from monitoring hard-to-access and restricted areas to tourism and heritage conservation. This technological convergence points toward a new paradigm in spatial data acquisition and modeling, in which low-cost and high-efficiency solutions become accessible to multiple sectors, democratizing the use of technologies that were previously restricted to specialized and high-cost equipment.

For future work, it is recommended to further investigate the analysis and interpretation of the collected data, considering different evaluation metrics and comparisons with other available technologies. Additionally, it is suggested to assess the economic and technical feasibility of integrating methods, such as combining photogrammetry and LiDAR, in order to achieve more comprehensive and accurate results.

References

AI PHOTO Editor Lab. *3D Scanner App*. 2024. Available at: https://apps.apple.com/us/app/id1419913995. Accessed: Mar. 30, 2026.

APPLE. *iPhone 14 Pro and iPhone 14 Pro Max*. Available at: https://www.apple.com/br/iphone-14-pro/. Accessed: Jun. 11, 2023.

BECKER, J. H.; CENTENO, J. A. S. Evaluation of filtering methods for point clouds derived from airborne laser scanning systems for DTM generation. *Brazilian Journal of Cartography*, v. 4, n. 65, p. 651–659, 2013.

CAZORLA, I. M. Arithmetic mean: a prosaic and complex concept. In: *Proceedings of the IX Seminar on Applied Statistics*, p. 1–14, 2003.

CLOUDCOMPARE. *CloudCompare Wiki – Introduction*. Available at: https://www.cloudcompare.org/doc/wiki/index.php/Introduction. Accessed: Jun. 11, 2023.

CPE. *GEODETIC TOTAL STATION SERIES G V2*. [s.l.: s.n.]. Available at: https://www.cpetecnologia.com.br/uploads/861fff29-022d-4637-a3c6-1166380885a1.pdf. Accessed: Jun. 11, 2023.

DESK, N. Here are six cool things you can do with the iPhone's LiDAR. Available at: https://surveyinggroup.com/here-is-the-super-cool-6-things-you-can-do-with-iphones-lidar/. Accessed: Jun. 11, 2023. *(Check if cited in text; otherwise, remove.)*

FAWZY, H. E. The accuracy of mobile phone cameras instead of high-resolution cameras in digital close-range photogrammetry. *International Journal of Civil Engineering & Technology (IJCIET)*, v. 6, n. 1, p. 76–85, 2015.

GARTNER. *IT Glossary*. Available at: http://www.gartner.com/itglossary/smartphotne. Accessed: Jun. 13, 2023. *(Not cited in text; consider removing.)*

GOMES, D. et al. Application of accurate photorealism for small monuments using close-range digital photogrammetry with smartphone cameras. *Brazilian Journal of Remote Sensing*, v. 1, n. 3, 2021.

GONÇALVES, E. M.; ALBARICI, F. L. Evaluation of positional accuracy of LiDAR sensors embedded in smartphones. *Brazilian Journal of Physical Geography*, v. 18, n. 2, p. 1247–1262, 2025. Available at: https://www.researchgate.net/profile/Fabio-Albarici/publication/389097672_Avaliacao_da_Acuracia_Posicional_de_Sensor_LiDAR_Incorporado_em_Smartph

ones/links/67b4e790207c0c20fa8d5387/Avaliacao-da-Acuracia-Posicional-de-Sensor-LiDAR-Incorporado-em-Smartphones.pdf.

HELMENSTINE, A. M. Absolute error or absolute uncertainty definition. *ThoughtCo*, Aug. 28, 2020. Available at: https://thoughtco.com/absolute-error-or-absolute-uncertainty-definition-604348.

JANICKA, J.; BŁASZCZAK-BĄK, W. Various scenarios of measurements using a smartphone with a LiDAR sensor in the context of integration with TLS point clouds. *Reports on Geodesy*, v. 119, p. 14–22, 2025. Available at: https://ieeexplore.ieee.org/abstract/document/10929822/.

LUETZENBURG, G.; KROON, A.; BJØRK, A. A. Evaluation of the Apple iPhone 12 Pro LiDAR for an application in geosciences. *Scientific Reports*, v. 11, 22221, 2021. Available at: https://doi.org/10.1038/s41598-021-01763-9.

MICELI, B. S. et al. Vertical evaluation of digital elevation models (DEMs) under different topographic configurations for medium and small scales. *Brazilian Journal of Cartography*, v. 63, n. 1, p. 191–201, 2011.

OLIVEIRA, A.; OLIVEIRA, T. A. *Elements of Descriptive Statistics*. 2011.

RABINOVICH, S. G. *Measurement Errors and Uncertainties: Theory and Practice*. Springer, 2006.

SANTOS, A. P. Evaluation of positional accuracy in spatial data using spatial statistics. PhD Thesis (Civil Engineering). Federal University of Viçosa, Viçosa, Brazil, 2010.

SAWANDI, H. et al. Smartphones as 3D mapping tools: a comparative study of LiDAR and photogrammetry techniques. In: *9th International Conference of SLAcJ*. Japan, 2026.

SILVA, R. P. et al. Evaluation of positional quality of point clouds obtained from terrestrial laser scanning (TLS). *Journal of Geosciences of the Northeast*, v. 10, n. 2, p. 284–297, 2024. DOI: 10.21680/2447-3359.2024v10n2ID36353. Available at: https://periodicos.ufrn.br/revistadoregne/article/view/36353. Accessed: Jun. 10, 2025.

SULEYMANOGLU, B. et al. Road infrastructure mapping using iPhone 14 Pro: an accuracy assessment. *The International Archives of the Photogrammetry, Remote Sensing and Spatial Information Sciences*, v. 48, p. 347–353, 2023.

TOMCZAK, K. et al. Estimating the volume of stacked wood using a dynamic conversion factor calculated by a LiDAR-based smartphone app. *International Journal of Forest Engineering*, p. 1–10, 2026. Available at: https://doi.org/10.1080/14942119.2026.2620234. Accessed: Mar. 30, 2026.